Long-Term Memory: A Natural Mechanism for the Clustering of Extreme Events and Anomalous Residual Times in Climate Records

Armin Bunde,[1] Jan F. Eichner,[1] Jan W. Kantelhardt,[1,2] and Shlomo Havlin[3]

[1]*Institut für Theoretische Physik III, Justus-Liebig-Universität Giessen, 35392 Giessen, Germany*

[2]*Fachbereich Physik und Zentrum für Computational Nanoscience, Martin-Luther-Universität Halle-Wittenberg, 06099 Halle (Saale), Germany*

[3]*Minerva Center and Department of Physics, Bar-Ilan University, Ramat-Gan 52900, Israel*

(Received 14 June 2004; published 31 January 2005)

We study the statistics of the return intervals between extreme events above a certain threshold in long-term persistent records. We find that the long-term memory leads (i) to a stretched exponential distribution of the return intervals, (ii) to a pronounced clustering of extreme events, and (iii) to an anomalous behavior of the mean residual time to the next event that depends on the history and increases with the elapsed time in a counterintuitive way. We present an analytical scaling approach and demonstrate that all these features can be seen in long climate records. The phenomena should also occur in heartbeat records, Internet traffic, and stock market volatility and have to be taken into account for an efficient risk evaluation.

DOI: 10.1103/PhysRevLett.94.048701 PACS numbers: 89.75.Da, 02.70.–c, 05.45.Tp, 92.70.Gt

Clustering of hazardous events has been reported in central Europe for the Middle Ages as well as for the last several decades (see [1–4] and references therein). A typical example is shown in Fig. 1(a), where the annual water levels of the Nile River [5], which exceed certain heights (quantiles), are shown for 663 years. Even by eye one can realize that the events are not distributed randomly but are arranged in clusters. A similar clustering was observed for extreme floods, winter storms, and avalanches in central Europe (see, e.g., Figs. 4.4, 4.7, 4.10, and 4.13 in [1], Fig. 66 in [2], and Fig. 2 in [4]). Model simulations show that greenhouse-gas induced global warming leads to an increased flood risk [6], which might explain the clustering of floods in the last several decades. However, an upward trend in the occurrence of the extreme floods has not been detected [4].

Here we show that the long-term correlations, inherent, e.g., in river flows [7] and temperature records [8], represent a natural mechanism for the clustering of the hazardous events. We find that the distribution of the return intervals strongly depends on the history and can be well approximated by a stretched exponential. In addition, the mean residual time to the next extreme event increases with the elapsed time and depends strongly on the history. We show that also this counterintuitive phenomenon can be seen in climate records with long-term memory. In order to avoid problems with seasonal trends, we focus on annual records. The data we consider are from the NOAA Paleoclimatological data bank [9].

Long-term correlated records $\{x_i\}, i = 1, \ldots, N$, with zero mean and unit variance, are characterized by an autocorrelation function $C_x(s) = \langle x_i x_{i+s} \rangle \equiv 1/(N-s) \times \sum_{i=1}^{N-s} x_i x_{i+s}$ that decays by a power law, $C_x(s) \sim s^{-\gamma}$, where the correlation exponent γ is between 0 and 1. To test the climate records for long-term correlations, we have employed the detrended fluctuation analysis (DFA2) [10,11]. In DFA2, one considers the cumulated sum $Y_i = \sum_{j=1}^{i} x_j$ and studies, in time windows of length s, the mean fluctuation $F(s)$ of Y_i around the best quadratic fit. For long-term correlated data, $F(s)$ scales as $F(s) \sim s^{\alpha}$, with $\alpha = 1 - \gamma/2$ (see, e.g., [8]). To standardize the records, we subtracted each record by its mean and divided by its variance. Figure 1(b) shows $F(s)$ for five representative climate records. In the double-logarithmic plot, the fluctuation functions are approximately straight lines, with slopes $\alpha = 0.95$, 0.85, 0.8, 0.73, and 0.6 (from top to bottom), yielding $\gamma = 0.1$ (Northern Hemisphere), 0.3 (Nile), 0.4 (New Mexico), 0.55 (Baffin), and 0.8 (Sacramento).

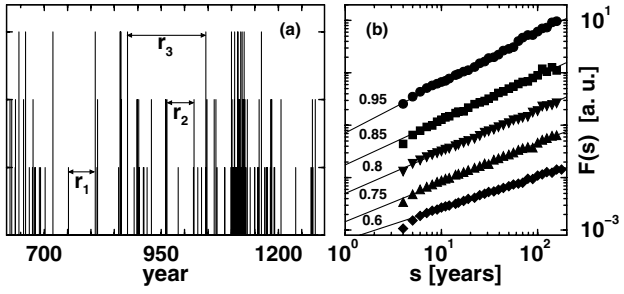

FIG. 1. (a) Illustration of the return intervals $r_q(l)$, $l = 1, \ldots, N_q$ for three equidistant threshold values q_1, q_2, q_3 for the water levels of the Nile at Roda (near Cairo, Egypt). One return interval for each quantile q is indicated by arrows. (b) DFA2 analysis for (i) the reconstructed Mann record of northern hemisphere temperatures (981 yr, circles) [12], (ii) the historical record of water levels of the Nile River [5] (663 yr, squares), (iii) the reconstructed precipitation record of New Mexico [13] (2129 yr, triangles down), (iv) the reconstructed temperature record of Baffin Island [14] (1241 yr, triangles up), and (v) the reconstructed river flow of the Sacramento River [15] (1109 yr, diamonds).

For describing the reoccurrence of rare events exceeding a certain threshold q, we investigate the statistics of the return intervals r_q between these events [see Fig. 1(a)]. It is known that for uncorrelated records (''white noise''), the return intervals are also uncorrelated and distributed according to the Poisson distribution, $P_q(r) = \frac{1}{R_q} \times \exp(-r/R_q)$, where R_q is the mean return interval for the given threshold q (see, e.g., [16]).

To see how this behavior changes in the presence of long-term correlations, we have used the Fourier-filtering technique (see, e.g., [17,18]) that generates linear long-term correlated records stochastically. As shown below, the behavior of the climate records is consistent with the behavior of these records, and nonlinearities are not needed to explain the properties studied here. Figure 2(a) shows the distribution $P_q(r)$ of the return intervals, for $\gamma = 0.5$, 0.3, and 0.1 and $q = 1.5$, 2.0, and 2.5, as a function of r/R_q. The result for the shuffled (uncorrelated) records is also shown. In both cases, $R_q P_q(r)$ depends only on the ratio r/R_q. This scaling is important, since it allows us to extrapolate the behavior at very large q values (rare events) from the behavior at small q values that are not rare and therefore have good statistics.

For the shuffled data, the distribution function is a simple exponential as expected. For the correlated data, we obtain a *stretched* exponential [19],

$$P_q(r) = \frac{a_\gamma}{R_q} \exp[-b_\gamma (r/R_q)^\gamma], \quad (1)$$

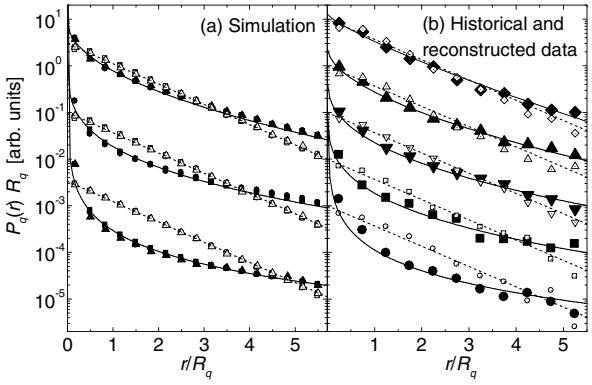

FIG. 2. (a) Distributions $P_q(r)$ of the return intervals r for the thresholds $q = 1.5$ ($R_q \approx 15$, squares), 2.0 ($R_q \approx 44$, circles), and 2.5 ($R_q \approx 161$, triangles) for simulated long-term correlated records with $\gamma = 0.5$ (top), 0.3 (middle), and 0.1 (bottom) (filled symbols) and for the corresponding shuffled data (open symbols). For the simulations, we used 1000 records of length $N = 2 \times 10^6$ for each value of γ. (b) Distributions $P_q(r)$ of the return intervals r for the five climate records considered in Fig. 1(b) with the same symbols, for both original data (filled symbols) and shuffled data (open symbols). The data have been averaged over all quantiles q with $R_q > 3$ yr and more than 50 return intervals. The lines are the theoretical curves following Eq. (1).

where the exponent γ is the correlation exponent, and the parameters a_γ and b_γ are independent of q.

Figure 2(b) shows the distribution function of the representative climate records from Fig. 1(b), and of the corresponding shuffled records. While the shuffled data clearly follow the Poisson distribution (dashed lines), the original data are close to a stretched exponential decay (continuous lines) with the γ values obtained from Fig. 1(b). The fluctuations of the results around the theoretical curves are due to the relatively short length of the records.

The form of the distribution (1) indicates that return intervals both well below and well above their average value R_q (which is independent of γ) are considerably more frequent for long-term correlated than for uncorrelated data. The equation does not quantify, however, if the return intervals themselves are arranged in a correlated or in an uncorrelated fashion, and if clustering of rare events may be induced by long-term correlations.

To study this question, we have evaluated the autocorrelation function $C_r(s) = \langle r_q(l) r_q(l+s) \rangle - R_q^2$ of the return intervals in simulated long-term correlated records. Representative results for $\gamma = 0.4$ and three q values ($q = 1.5$, 1.75, and 2.0) are shown in Fig. 3(a). In the double-logarithmic presentation, the three curves are parallel straight lines with slopes -0.4. This result suggests that also the return intervals are long-term power-law correlated, with the same exponent γ as the original record.

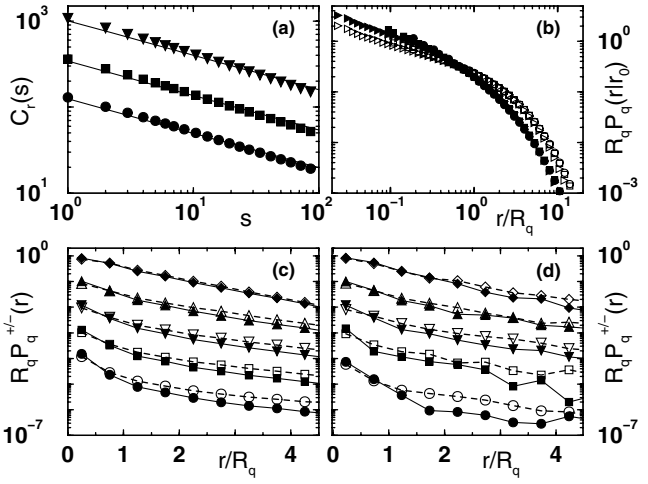

FIG. 3. (a) Autocorrelation function $C_r(s)$ of the return intervals for $q = 1.5$ (circles), 1.75 (squares), and 2.0 (triangles) for simulated long-term correlated records with $\gamma = 0.4$. (b) Conditional distribution function $P_q(r|r_0)$ versus r/R_q for $\gamma = 0.4$ and $q = 1.5$ (circles), 1.75 (squares), and 2.0 (triangles), for $r_0 = R_q/4$ (open symbols) and $r_0 = 4R_q$ (full symbols). (c),(d) $R_q P_q^+(r)$ (open symbols) and $R_q P_q^-(r)$ (full symbols), averaged over all r_0 above and below the median return interval, respectively, versus r/R_q for (c) artificial records and (d) the five climate records from Fig. 1(b). The artificial data in (c) have the same γ values and mean record lengths as the climate records; we studied 1000 records of size $N = 1250$.

Accordingly, large and small return intervals are not arranged in a random fashion but are expected to form clusters.

As a consequence, the probability of finding a certain return interval r depends on the value of the preceding interval r_0, and this effect has to be taken into account in predictions and risk estimations. Figure 3(b) shows, for two values of r_0/R_q, the (conditional) distribution function $P_q(r|r_0)$ that a return interval r_0 is followed by a return interval r, as a function of r/R_q, for $\gamma = 0.4$ and $q = 1.5$, 2.0, and 2.5. The plot clearly displays the dependence on r_0 due to the long-term memory. Since for fixed r_0/R_q all data points collapse to a single curve, the conditional distribution function scales as $P_q(r|r_0) = (1/R_q)f(r/R_q, r_0/R_q)$.

The dependence on the preceding return interval r_0 is a direct manifestation of the long-term memory. To reveal this behavior in the relatively short climate records, it is necessary to improve the statistics by integrating over a certain range of r_0 values. Here, we consider the median r_q^* of the return intervals and study the conditional distributions $P_q^-(r)$ and $P_q^+(r)$ of all those intervals that directly follow return intervals r_0 either below or above r_q^*, respectively. Figures 3(c) and 3(d) show that the results for the climate records (d) are in good agreement with those of the corresponding simulated records (c). As expected, the difference between P_q^+ and P_q^-, i.e., the dependence of the distribution function on the history, becomes more pronounced with decreasing value of γ, i.e., increasing long-term memory. The large fluctuations for the climate records are due to their limited size.

The conditional distribution function $P_q(r|r_0)$ is a basic quantity, from which the relevant quantities in risk estimations can be derived [16]. For example, the first moment of $P_q(r|r_0)$ is the average value $R_q(r_0)$ of those return intervals that directly follow r_0. By definition, $R_q(r_0)$ is the expected waiting time to the next event, when the two events before were separated by r_0. The more general quantity is the expected waiting time $\tau_q(x|r_0)$ to the next event, when the time x has elapsed. For $x = 0$, $\tau_q(0|r_0)$ is identical to $R_q(r_0)$. In general, $\tau_q(x|r_0)$ is related to $P_q(r|r_0)$ by

$$\tau_q(x|r_0) = \int_x^\infty (r - x) P_q(r|r_0) dr \Big/ \int_x^\infty P_q(r|r_0) dr. \quad (2)$$

For uncorrelated records, $\tau_q(x|r_0)/R_q = 1$ (except for discreteness effects that lead to $\tau_q(x|r_0)/R_q > 1$ for $x > 0$; see [20]). Because of the scaling of $P_q(r|r_0)$, we expect that also $\tau_q(x|r_0)/R_q$ scales with r_0/R_q and x/R_q. Figure 4(a) shows that this is indeed the case. The data collapse for each value of x/R_q confirms the scaling property. The figure clearly displays the effect of the long-term memory: Small and large return intervals are more likely to be followed by small and large ones, respectively, and hence $\tau_q(0|r_0)/R_q \equiv R_q(r_0)/R_q$ is well below (above) one for

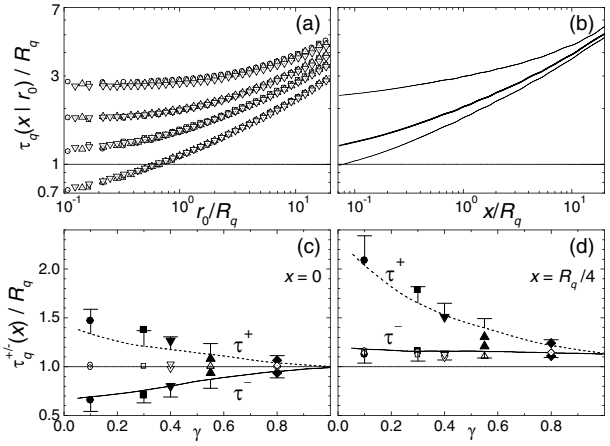

FIG. 4. (a) Mean residual time to the next event $\tau_q(x|r_0)$ (in units of R_q) versus r_0/R_q for four q values ($q = 1.0$, 1.25, 1.5, and 1.75, different symbols) and four values of the elapsed time x since the last event ($x/R_q = 0$, 0.25, 1, and 4, from bottom to top). (b) Mean residual time $\tau_q(x|r_0)$ as a function of x/R_q, for $r_0/R_q = 1/8$ (lower curve) and $r_0/R_q = 8$ (upper curve). The middle curve represents the mean residual time averaged over all r_0. (c),(d) Mean residual times $\tau_q^-(x)$ (full line) and $\tau_q^+(x)$ (dashed line), averaged over all r_0 below and above the median return interval, respectively, for (c) $x = 0$ and (d) $x = R_q/4$. The symbols are for the five climate records from Fig. 1(b), for both original data (filled symbols) and shuffled data (open symbols). For obtaining the curves in (a),(b) we used the same statistics as in Figs. 2(a) and 3(a) and 3(b), and for the theoretical curves in (c),(d) and the error bars we used the same statistics as in Fig. 3(c).

r_0/R_q well below (above) one. With increasing x, the expected residual time to the next event increases, as is also shown in Fig. 4(b), for two values of r_0 (top and bottom curve). Note that only for an infinite long-term correlated record, the value of $\tau_q(x|r_0)$ will increase indefinitely with x and r_0. For real (finite) records, there exists a maximum return interval which limits the values of x, r_0, and $\tau_q(x|r_0)$. The middle curve shows the expected residual time averaged over all r_0, i.e., the unconditional residual time. In this case, the interval between the last two events is not taken explicitly into account, and the slower-than-Poisson decrease of the unconditional distribution function $P_q(r)$, Eq. (1), leads to the anomalous increase of the mean residual time with the elapsed time [20]. Very recently, this approach (average over r_0) has been applied successfully to worldwide earthquake records [21]. For the case of long-term correlated records, however, like the hydroclimate records discussed here, the large differences between the three curves in Fig. 4(b) suggest that for an efficient risk estimation, also the previous return interval has to be taken into account, and not only the distribution of the return intervals.

To reveal this intriguing behavior in the relatively short observed and reconstructed records, we improve the sta-

tistics [similar to Figs. 3(c) and 3(d)] by studying the mean expected residual times $\tau_q^-(x)$ and $\tau_q^+(x)$ for r_0 below and above the median r_q^*, respectively. For uncorrelated data, both quantities are identical and coincide with R_q.

Figure 4(c) shows $\tau_q^+(0)/R_q$ and $\tau_q^-(0)/R_q$ versus γ for simulated records (lines) and the five representative climate records (symbols). The difference between τ_q^+ and τ_q^- becomes more pronounced with decreasing value of γ, i.e., increasing long-term memory. The results for the climate records are in good agreement with the theoretical curves. The same comparison for $x/R_q = 1/4$ instead of $x = 0$ is shown in Fig. 4(d). The behavior is qualitatively different: while $\tau_q^-(0)/R_q$ increases with increasing γ, $\tau_q^-(R_q/4)/R_q$ is rather constant. Again, the agreement between simulated and real records is quite satisfactory, revealing the strong effect of memory in the hydroclimate records that also results in the clustering of the extreme events. To show the significance of the results, we also analyzed the corresponding shuffled data [as in Fig. 2(b)]. We obtained $\tau_q^+(0)/R_q \approx \tau_q^-(0)/R_q \approx 1$ and $\tau_q^+(R_q/4)/R_q \approx \tau_q^-(R_q/4)/R_q \approx 1.1$. In the second case, the shuffled data (following the Poisson distribution) show a slight increase of the residual time (1.1 instead of 1). This is a finite size effect that already has been noticed in [20].

In summary, we have shown that the long-term persistence inherent in hydroclimate records represents a natural mechanism for the clustering of the hazardous events seen in central Europe in the Middle Ages as well as in the past several decades. We also found that, as a consequence of the long-term memory, the mean residual time to the next event increases with the elapsed time and depends strongly on the previous return interval. We have demonstrated that also this counterintuitive phenomenon can be seen in long-term climate records. We note that both features, the clustering of the extreme events as well as the anomalous behavior of the mean residual times to the next event, should also appear in heartbeat records [11,22], Internet traffic [23], and stock market volatility [24] that are known to exhibit long-term memory.

This work has been supported by the Bundesministerium für Bildung und Forschung and the Israel Science Foundation.

[1] C. Pfister, *Wetternachhersage. 500 Jahre Klimavariationen und Naturkatastrophen 1496–1995* (Verlag Paul Haupt, Bern, 1998).
[2] R. Glaser, *Klimageschichte Mitteleuropas* (Wissenschaftliche Buchgesellschaft, Darmstadt, 2001).
[3] W. Soon and S. Baliunas, Climate Res. **23**, 89 (2003).
[4] M. Mudelsee, M. Börngen, G. Tetzlaff, and U. Grünwald, Nature (London) **425**, 166 (2003).
[5] Data obtained from http://sunsite.univie.ac.at/statlib/S/beran; see also B. Whitcher *et al.*, Water Resour. Res. **38**, 1054 (2002).
[6] J. H. Christensen and O. B. Christensen, Nature (London) **421**, 805 (2003).
[7] H. E. Hurst *et al.*, *Long-Term Storage: An Experimental Study* (Constable & Co. Ltd., London, 1965); B. B. Mandelbrot and J. R. Wallis, Water Resour. Res. **5**, 321 (1969); I. Rodriguez-Iturbe *et al.*, *Fractal River Basins—Change and Self-Organization* (Cambridge University Press, Cambridge, 1997).
[8] E. Koscielny-Bunde *et al.*, Phys. Rev. Lett. **81**, 729 (1998); J. D. Pelletier and D. L. Turcotte, Adv. Geophys. **40**, 91 (1999); R. O. Weber and P. Talkner, J. Geophys. Res. Atmos. **106**, 20131 (2001); J. F. Eichner *et al.*, Phys. Rev. E **68**, 046133 (2003).
[9] NOAA Paleoclimatology Program, http://www.ngdc.noaa.gov/paleo/recons.html.
[10] C.-K. Peng *et al.*, Phys. Rev. E **49**, 1685 (1994).
[11] A. Bunde, S. Havlin, J. W. Kantelhardt, T. Penzel, J.-H. Peter, and K. Voigt, Phys. Rev. Lett. **85**, 3736 (2000).
[12] M. E. Mann, R. S. Bradley, and M. K. Hughes, Geophys. Res. Lett. **26**, 759 (1999).
[13] H. D. Grissino-Mayer, *Tree Rings, Environment, and Humanity*, edited by J. S. Dean, D. M. Meko, and T. W. Swetnam, *Radiocarbon 1996* (Department of Geosciences, The University of Arizona, Tucson, 1996), pp. 191–204.
[14] J. J. Moore, K. A. Hughen, G. H. Miller, and J. T. Overpeck, J. Paleolimnology **25**, 503 (2001).
[15] D. M. Meko, M. D. Therrell, C. H. Baisan, and M. K. Hughes, J. Am. Water Resour. Assoc. **37**, 1029 (2001).
[16] H. v. Storch and F. W. Zwiers, *Statistical Analysis in Climate Research* (Cambridge University Press, Cambridge, 1999).
[17] D. L. Turcotte, *Fractals and Chaos in Geology and Geophysics* (Cambridge University Press, Cambridge, 1992).
[18] H. A. Makse *et al.*, Phys. Rev. E **53**, 5445 (1996).
[19] When considering the (different) problem of zero-level crossings in long-term correlated data with Gaussian noise, it has been proven by G. F. Newell and M. Rosenblatt in Ann. Math. Statist. **33**, 1306 (1962) that the probability of having no zero-level crossing after t time steps is bounded from above by a stretched exponential.
[20] D. Sornette and L. Knopoff, Bull. Seismol. Soc. Am. **87**, 789 (1997).
[21] A. Corral, Phys. Rev. Lett. **92**, 108501 (2004).
[22] C.-K. Peng, J. Mietus, J. M. Hausdorff, S. Havlin, H. E. Stanley, and A. L. Goldberger, Phys. Rev. Lett. **70**, 1343 (1993).
[23] W. E. Leland, M. S. Taqqu, W. Willinger, and D. V. Wilson, IEEE/ACM Trans. Networking **2**, 1 (1994); V. Paxson and S. Floyd, IEEE/ACM Trans. Networking **3**, 226 (1995).
[24] Y. Liu, P. Gopikrishnan, P. Cizeau, M. Meyer, C.-K. Peng, and H. E. Stanley, Phys. Rev. E **60**, 1390 (1999).